Title

Epidermal growth factor receptor signaling in precancerous keratinocytes promotes neighboring head and neck cancer squamous cell carcinoma cancer stem cell-like properties and phosphoinositide 3-kinase inhibitor insensitivity.

Journal

Molecular Carcinogenesis, 61(7)

Authors

Nguyen, Khoa
Keith, Madison
Keysar, Stephen
et al.

Publication Date

2022-07-01

DOI

10.1002/mc.23409

Peer reviewed

HHS Public Access

Author manuscript

Mol Carcinog. Author manuscript; available in PMC 2023 July 01.

Published in final edited form as:

Mol Carcinog. 2022 July ; 61(7): 664–676. doi:10.1002/mc.23409.

Epidermal growth factor receptor signaling in precancerous keratinocytes promotes neighboring head and neck cancer squamous cell carcinoma cancer stem cell-like properties and phosphoinositide 3-kinase inhibitor insensitivity

Khoa A. Nguyen[1],

Madison J. Keith[1],

Stephen B. Keysar[2],

Spencer C. Hall[1],

Anamol Bimali[1],

Antonio Jimeno[2],

Xiao-Jing Wang[1,3],

Christian D. Young[1,#]

[1)]Department of Pathology, University of Colorado Anschutz Medical Campus. Aurora, CO

[2)]Division of Medical Oncology, Department of Medicine, University of Colorado Anschutz Medical Campus, Aurora, CO

[3)]Veterans Affairs Medical Center, VA Eastern Colorado Health Care System, Aurora, Colorado.

Abstract

Head and neck squamous cell carcinoma (HNSCC) is commonly associated with tobacco and alcohol consumption that induce a “precancerous field,” with phosphoinositide 3-kinase (PI3K) signaling being a common driver. However, the preclinical effectiveness of PI3K inhibitors has not necessarily translated to remarkable benefit in HNSCC patients. Thus, we sought to determine how precancerous keratinocytes influence HNSCC proliferation, cancer stem cell (CSC) maintenance, and response to PI3K inhibitors. We used the NOK keratinocyte cell line as a model of preneoplastic keratinocytes because it harbors two frequent genetic events in HNSCC, *CDKN2A* promoter methylation and *TP53* mutation, but does not form tumors. NOK cell co-culture or NOK cell conditioned media promoted HNSCC proliferation, PI3K inhibitor resistance, and CSC phenotypes. SOMAscan targeted proteomics determined the relative levels of >1,300 analytes in the media conditioned by NOK cells and HNSCC cells ± PI3K inhibitor. These results demonstrated that NOK cells release abundant levels of ligands that activate EGFR and FGFR, two receptor tyrosine kinases with oncogenic activity. Inhibition of EGFR, but not FGFR, blunted PI3K inhibitor resistance and CSC phenotypes induced by NOK cells. Our results demonstrate that precancerous keratinocytes can directly support neighboring HNSCC by activating EGFR. Importantly, PI3K inhibitor sensitivity was not necessarily a cancer cell-intrinsic property, and the

[#]Corresponding Author: Christian D. Young, 12800 E. 19th Avenue, Aurora, CO 80045, Mail stop 8104, Phone (303) 724-3093; Fax (303) 724-4730, christian.young@cuanschutz.edu.

tumor microenvironment impacts therapeutic response and supports CSCs. Additionally, combined inhibition of EGFR with PI3K inhibitor diminished EGFR activation induced by PI3K inhibitor and potently inhibited cancer cell proliferation and CSC maintenance.

Keywords

PI3K; EGFR; HNSCC; Cancer stem cell; resistance; squamous cell carcinoma

INTRODUCTION

Head and neck squamous cell carcinoma (HNSCC) is the sixth most common cancer type, accounting for over 890,000 new cases and approximately 450,000 deaths each year worldwide[1]. The sensitive anatomy of the head and neck is important for speech, taste, smell, breathing, swallowing, chewing, etc. meaning that surgery/irradiation of the head and neck region to treat cancer often produces serious quality of life concerns in addition to the morbidity caused by the tumor itself. Intertwined with this already sensitive anatomy is a “cancerized field” of mucosa surrounding the carcinoma, often induced by tobacco or alcohol consumption[2–5]. Precancerous cells may eventually form tumors and persist as an HNSCC-adjacent field after establishment of a tumor, however, the cancerized field is often grossly undetectable[6]. Importantly, the cancerized field can drive relapse and secondary tumor formation after primary tumor removal[3,4]. The significant morbidity associated with HNSCC demands evaluation of innovative therapeutic options. As such, defining targetable mechanisms by which the cancerized field drives tumor cell progression is critical to decreasing relapse, augmenting surgery success rate, and preventing potential tumor emergence in high-risk patients.

Mutations/amplifications within components of the phosphoinositide-3-kinase (PI3K) signaling pathway are present in >40% of HNSCC tumors, making the PI3K pathway the most frequently activated oncogenic signaling pathway in HNSCC[7–10]. Additionally, another >25% of tumors harbor amplification of EGFR, FGFR1, ERBB2 or IGF1R receptor tyrosine kinases[10], all of which lead to activation of PI3K. Thus, development of PI3K inhibitors and their investigation in clinical trials are being intensely pursued in HNSCC as well as other cancer types. While some clinical trials suggest that tumors with PI3K genomic alterations may preferentially benefit from PI3K targeted therapeutics, others demonstrate effectiveness in both PI3K wild type and PI3K mutated subsets[11–13]. For example, a recent clinical trial adding PI3K inhibitor to paclitaxel treatment improved progression free survival in recurrent HNSCC patients regardless of PI3K pathway mutation status in tumors [11]. In HNSCC patient-derived xenografts and cell lines, tumors with activating *PIK3CA* alterations demonstrated favorable response to PI3K inhibitors[7,14], however *PIK3CA* alterations have not been a ubiquitous biomarker of response, since many oncogenic activities induce PI3K without mutation of core PI3K components[15,16]. Determining the biological and signaling consequences of PI3K inhibitors is therefore critical to guiding future trials and optimizing therapeutic combinations while biomarkers predicting patients who may benefit from PI3K inhibitors are established.

Cancer stem cells (CSC) are a critical therapeutic target due to their ability to resist treatment and repopulate tumor heterogeneity[17,18]. For this reason, identifying pathways driving their survival and growth is imperative. One promising CSC driver is the PI3K signaling pathway, which is highly active in most HNSCCs. Notably, PI3K induces SCCs when activated in stem cells and contributes to HNSCC CSC maintenance[7,19,20]. In addition to promoting tumor cell proliferation and survival, PI3K signaling has also been shown to activate CSC properties, however, recent studies report mixed sensitivities of CSCs to PI3K inhibition[20,21]. Consequently, determining the tumor-specific factors, such as the tumor microenvironment (TME), that augment or inhibit PI3K inhibitor efficacy is critical to maximizing the potential of using this candidate treatment strategy.

In this study, we investigated potential ways in which preneoplastic keratinocytes affect neighboring HNSCC using immortalized oral keratinocytes (NOK cells) as a model of the HNSCC-adjacent field. We chose NOK cells as our model of the precancerous field since they harbor two common genetic alterations in HNSCC and preneoplastic mucosa, mutant *TP53* and *CDKN2A* promoter methylation, but do not form tumors[22,23]. We report pro-tumor effects such as increased proliferation, resistance to PI3K inhibition, and CSC-like properties when HNSCC cells are co-cultured with preneoplastic keratinocytes. Using a proteomics approach, we identified soluble factors secreted by our model of preneoplastic mucosa responsible for these effects. Furthermore, we report the dependence of these effects on epidermal growth factor receptor (EGFR) ligands, which can be targeted using an EGFR inhibitor. Our study provides novel insights toward characterizing the contributions of the cancerized field to HNSCC progression and offers proof-of-principle for leveraging this component of the TME to improve precision medicine and better understand how the TME contributes to PI3K inhibitor insensitivity and CSC maintenance.

MATERIALS & METHODS

Reagents-

All cell culture reagents (including media and sera) were obtained from Gibco unless otherwise noted. BKM120, Erlotinib, and AZD4547 were purchased from MedChemExpress and resuspended in DMSO to a stock concentration of 10 mM. BKM120 was used at a final concentration of 1 μM. Erlotinib and AZD547 were used at a final concentration of 0.5 μM. IncuCyte NucLight red lentivirus was purchased from Essen Biosciences. SMARTpool ON-TARGETplus siRNA pools (of four different siRNA duplexes) were purchased from Dharmacon (Negative control, non-targeting: D-001810–10-05; Sox2 targeted: L-011778–00-0005). Antibodies are listed in Table 1.

Cell culture-

CAL27 cells were purchased from American Type Culture Collection. UMSCC1 cells were provided previously[24]. NOKSI cells, herein referred to as “NOK cells”, were provided as a gift by Dr. Gutkind (University of California, San Diego). Cell line identities were confirmed by STR profiling (The Centre for Applied Genomics, The Hospital for Sick Children, Toronto) and cross-referenced to published STR profiles[22,25]. All culture reagents were obtained from Gibco unless otherwise noted. CAL27 and UMSCC1

were routinely maintained in DMEM containing 10% fetal bovine serum (FBS) and 1x primocin (antibiotic; Invivogen). NOK cells were routinely maintained in Keratinocyte SFM supplemented with 2 ng/mL EGF. CAL27 and UMSCC1 were infected with IncuCyte NucLight red lentivirus (Sartorius) using 8 μg/mL polybrene to aid virus transduction. Stable expression of nuclear red expressing cells was selected with 10 μg/mL bleomycin sulfate and verified by fluorescent microscopy.

All experiments were performed in “low serum media”: DMEM containing 1% charcoal stripped FBS and 1x primocin, to minimize FBS growth factor effects. B27 supplement was added (at a final 1x concentration) in tumorsphere assays. In co-culture experiments, 1,000 of each cell type were seeded to 96 well plates in low serum media and allowed to adhere overnight before inhibitors were added and cell number monitored by IncuCyte Zoom live cell imaging at the University of Colorado Cell Technologies Shared Resource. In conditioned media treatment experiments, fully confluent plates of NOK cells were washed twice with PBS and incubated in low serum media overnight. The serum-starved NOK cells were treated with fresh low serum media containing 2 μM BKM120 or DMSO for 24 hr, media then harvested and filtered through a 0.45 micron PES filter. Parallel plates without cells were treated identically to generate unconditioned control media. NOK-conditioned and unconditioned media were applied to recipient HNSCC cultures in low serum media such that donor media was half the volume of the culture (and drug concentrations cut in half). In tumorsphere formation assays, 200 cells were seeded in ultra-low attachment 96 well plates (Corning), treated as indicated, and cultured 10–14 days to allow tumorsphere formation. Whole well images were captured using IncuCyte Zoom instrument and tumorspheres larger than 50 microns were counted in each well and averaged across replicates.

SOMAscan 1.3k proteomic analysis-

One million CAL27 or NOK cells were seeded to wells of 6 well plates in complete media and allowed to adhere overnight. The next day the cells were washed with PBS then incubated overnight in serum-free DMEM followed by 24 hr incubation in serum free DMEM containing 1 μM BKM120 or DMSO. Conditioned media were harvested and submitted for SOMAscan 1.3k analysis at the University of Colorado Genomics and Microarray Shared Resource. The raw data were normalized to account for hybridization variation and standard quality control procedures for internal controls and samples was performed using the standard SomaLogic platform and criteria to scale and filter the data. The hybridization normalized relative fluorescent units (RFU) for each analyte and each sample are presented graphically and by spreadsheet.

SRB assay-

To assess relative cell abundance, one 96 well plate of cancer cells was fixed on day 0 and another plate was treated as described and incubated 3 days before cells were fixed with 10% TCA for 30 min at 4°C, then washed five times with water and dried. Relative protein per well in fixed, dried plates was assessed by SRB Assay: 100 μL 0.4% SRB diluted in 1% acetic acid was applied to each well for 1 hr before being washed five times with 1% acetic acid to remove unbound dye then plates were dried. Wells of stained plates

(including no cell blank controls) were resuspended with 100 μL 10 mM Tris, shaken for 1 min on an orbital plate shaker, and the absorbance of each well measured at 560 nM using a plate reading spectrophotometer. The day 3 absorbance values were normalized to the pretreatment day 0 absorbance values to determine relative cell abundance.

SOX2 activity and CD44 expression assays-

SORE6-mCMVp-dsCopGFP ("SORE6-GFP") is a vector that has six replicates of the *SOX2/OCT4* response element of the *NANOG* promoter upstream of a destabilized *copGFP* reporter to permit interrogation of SOX2 and/or OCT4 transcriptional activity by GFP expression[26]. Lentivirus was generated by co-transfecting HEK293T with 3.6 μg SORE6-GFP plasmid, 2.7 μg pΔ8.9 (encoding *Gag* and *Pol*) and 1.7 μg pVSVG envelope using the calcium phosphate method. Transfected packaging cell were provided fresh media 24 hr post-transfection and virus containing supernatants were collected 48 hr post-transfection. 1.5 mL of virus-containing supernatant was mixed with 0.5 mL UMSCC1 or CAL27 cells and 8 μg/mL polybrene in 6 well plates. Transduced cells were selected with 1 μg/mL puromycin. Expression of the inducible GFP reporter was validated by flow cytometry detection of GFP after transfection with non-targeting control or SOX2-targeted siRNA. siRNA SMARTpools (Dharmacon) were transfected into CAL27-SORE6-GFP or UMSCC1-SORE6-GFP cells at a final concentration of 25 nM using Lipofectamine RNAiMAX (Invitrogen) at a ratio of 1.2 μL Lipofectamine RNAiMAX per 1.0 μL 20 μM stock siRNA. Three days post-transfection cells were lysed to validate SOX2 knockdown by western blot or dissociated into single cells for flow cytometry analysis.

For flow cytometry detection of $CD44^{high}$ or SOX2 reporter activity, 200,000 CAL27 or UMSCC1 cells (or CAL27-SORE6-GFP or UMSCC1-SORE6-GFP) were seeded in ultra-low attachment 6 well plates, a density at which all cultures form tumorspheres in three days. Tumorspheres were dissociated in Accutase cell dissociation reagent (Thermo Fisher). For CD44 detection, cells were then stained with CD44-APC antibody diluted in flow cytometry buffer (FCB; PBS containing 2% BSA) for 30 minutes at 4 degrees. For detecting SOX2 reporter activity, tumorspheres were dissociated and washed with FCB followed by flow cytometry analysis to detect the GFP reporter. Flow cytometry was performed using a Gallios Flow Cytometer (Beckman Coulter) and Kaluzu analysis software at the University of Colorado Flow Cytometry Core Facility.

Immunoblot analysis-

Cell monolayers were washed with PBS, lysed with RIPA lysis buffer (Cell Signaling Technologies) containing Complete Protease Inhibitor Cocktail (Roche), scraped using a plastic cell lifter and transferred to microfuge tubes. Whole cell lysates were clarified by centrifugation at maximum speed at 4°C for 10 min. Clarified lysates were collected to new tubes and insoluble pellets discarded. Protein concentrations of individual lysates were determined by BCA assay (Pierce) and lysate protein concentrations were normalized with lysis buffer and diluted with 4xNuPAGE LDS sample buffer (Invitrogen) containing 5% 2-mercaptoethanol. Equal quantities of protein per lane were resolved using NuPAGE Bis-Tris protein gels (Invitrogen) and transferred to Nitrocellulose (BioRad) in Tris-Glycine-Methanol transfer buffer. Membranes were blocked in 5% non-fat dry milk reconstituted

in TBST and then incubated overnight with primary antibodies detailed in Table 1 diluted in TBST containing 5% BSA. Primary antibodies were detected with species-specific HRP-conjugated secondary antibodies (Cell Signaling Technologies) and then developed with enhanced chemiluminescence substrate (Pierce) and X-ray film.

Statistical analysis-

Statistics were performed using Graphpad Prism software and the statistical test used is detailed in each figure legend. Repeated measure ANOVA with Tukey's multiple comparison test was utilized to analyze repeated measures, one way ANOVA with Tukey's multiple comparison test was used to analyze one variable experiments, and two-way ANOVA with Tukey's multiple comparison tests was used to analyze two variable experiments.

RESULTS

Precancerous keratinocytes decrease neighboring HNSCC PI3K inhibitor sensitivity while increasing features of HNSCC cancer stem cells

To model HNSCC adjacent to a precancerous field, we utilized two human oral cancer cell lines, CAL27 and UMSCC1, and a precancerous keratinocyte cell line, NOK. NOK cells harbor *TP53* mutation and *CDKN2A* methylation[22], two frequent events in HNSCC progression and preneoplasia[23], but do not form tumors, justifying their use as a model of precancerous keratinocytes. We labeled the two HNSCC cell lines with a nuclear red reporter so the number of nuclear red HNSCC cells could be quantified over time using IncuCyte Zoom live cell imaging system independent of co-cultured cells. In low serum media, the nuclear red HNSCC cells proliferated for 48–72 hours before declining in abundance (Fig. 1A–B). When co-cultured with NOK cells, CAL27 and UMSCC1 cells proliferated more robustly than when co-cultured with unlabeled CAL27 or UMSCC1 cells, respectively (Fig. 1A–B, open triangle vs open square). Co-cultures were treated with pan-class I PI3K inhibitor BKM120 or DMSO to determine whether precancerous keratinocytes influence HNSCC PI3K inhibitor sensitivity. Treatment with BKM120, reduced proliferation rates of both CAL27 and UMSCC1 cells (Fig. 1A–B, closed triangle). However, when co-cultured with NOK cells, both HNSCC cell lines demonstrated enhanced survival and reduced BKM120 sensitivity (Fig 1A–B, closed squares). To determine whether soluble factors from NOK cells mediate these effects, we harvested the conditioned media of NOK cells treated with DMSO or BKM120 using unconditioned DMSO- or BKM120-containing media as controls. Similar to co-culture, CAL27 and UMSCC1 cells were both sensitive to BKM120 in unconditioned media, but not BKM120 in NOK conditioned media (Fig. 1C–D). Importantly, recipient CAL27 and UMSCC1 cells both demonstrated identical levels of reduced P-Akt when treated with BKM120 from unconditioned media or from NOK conditioned media suggesting BKM120 is still active in cells treated with NOK conditioned media (Fig. 1E).

Because tumor aggressiveness and therapy resistance are associated with cancer stem cell-like features, we next determined how NOK cells influenced markers of CSCs. Self-renewal associated with tumorsphere formation is one assay for CSCs. CAL27 cells are unable

to form tumorspheres in unconditioned media, but readily formed spheres when treated with the conditioned media of NOK cells. Interestingly, CAL27 cells form tumorspheres even when treated with conditioned media of BKM120 treated NOK cells (Fig. 2A–B). Similarly, UMSCC1 tumorsphere formation was increased 3-fold by NOK conditioned media compared to unconditioned media and tumorspheres formed in the presence of conditioned media from BKM120 treated NOK cells, albeit at a reduced rate and size compared to DMSO (Fig. 2A–B). Several cell surface markers have been associated with CSCs. One such marker, $CD44^{high}$ expression[20], was increased in HNSCC tumorspheres resulting from NOK conditioned media treatment (Fig. 2C). HNSCC CSCs are also associated with increased ALDH and SOX2 activity. While we did not observe an increase in ALDH activity as measured by aldefluor assay (data not shown), the media conditioned by NOK cells increased SOX2 activity in recipient HNSCC as measured by a SOX2-response element GFP reporter (Fig. 2D). siRNA-mediated knockdown of SOX2 reduced basal and NOK conditioned media-induced Sox2 reporter activity (Supp. Fig. S1) suggesting this reporter is in fact responding to SOX2 activity. Thus, soluble factors from NOK cells can also mediate SOX2-dependent CSC properties in recipient CAL27 and UMSCC1 cells.

The CSC promoting activity of conditioned media from NOK cells treated with BKM120 was surprising given the role of PI3K signaling in maintaining CSC traits[20,27]. Thus, we wanted to determine if the media conditioned by NOK cells in the presence of BKM120 has different activity than NOK conditioned media later “spiked” with BKM120. Indeed, only the media conditioned by NOK cells cultured with BKM120 could induce tumorsphere formation in recipient HNSCC cells, while media conditioned by NOK cells that had BKM120 added after conditioning failed to induce tumorsphere formation (Supp. Fig. S2). Thus, the ability of NOK cells to convey PI3K inhibitor resistance and CSC traits to HNSCC is a result of the NOK cell response to PI3K inhibitor and release of factors into the media.

NOK cells release elevated levels of FGFR and EGFR family ligands

To determine which soluble factors from NOK cells are mediating CSC properties and PI3K inhibitor insensitivity in recipient HNSCC cells, we harvested the conditioned media of NOK cells treated with DMSO or BKM120 and analyzed >1,300 analytes using SOMAscan targeted proteomics platform. The conditioned media of CAL27 cells treated with DMSO or BKM120 was used as a control. The relative levels of all 1,300 analytes in each sample are presented in supplementary table 1, and striking changes included receptor tyrosine kinase ligands. Of the 17 FGFR ligands in the panel, 16 were higher in NOK cells than CAL27 cells and were increased in BKM120-treated samples compared to DMSO (Fig. 3A; supplementary table 1). The only ligand that did not follow this pattern was FGF1 (Fig. 3A). All six EGFR family ligands in the panel were more highly released by NOK than CAL27 and increased by BKM120 treatment (Fig. 3B). ELISA for FGF2 confirmed that this FGFR ligand is most highly released by NOK (compared to CAL27 or UMSCC1) and is increased by BKM120 treatment (Fig. 3C). Levels of ligands for PDGFR and VEGFR family RTKs did not follow these trends (Fig. 3D–E), suggesting ligands of FGFR and/or EGFR may play a functional role in the activities conferred by NOK conditioned media on recipient HNSCC cells.

Inhibition of EGFR, but not FGFR, blunts PI3K inhibitor insensitivity and CSC properties conferred to HNSCC cells by NOK cells

Because multiple EGFR family ligands activate four different EGFR family receptors, FGFR family ligands activate four different FGFR family receptors, and multiple ligands were released by NOK cells, we used erlotinib to inhibit EGFR[28] and AZD4547 to inhibit FGFR1–3[29]. The induction of $CD44^{high}$ by NOK conditioned media was abolished by erlotinib in both recipient cell lines while a modest effect of AZD4547 on $CD44^{high}$ was observed in UMSCC1, but not CAL27 (Fig. 4A). The induction of SOX2 reporter activity by NOK conditioned media in recipient CAL27 and UMSCC1 was decreased by erlotinib, but not AZD4547 (Fig. 4B). Erlotinib, and to a lesser extent AZD4547, blunted the BKM120 insensitivity conferred to CAL27 and UMSCC1 by co-culture with NOK cells (Fig. 5A) or application of NOK conditioned media to recipient HNSCC cells (Fig. 5B). The tumorsphere formation activity conferred to recipient CAL27 or UMSCC1 cells by NOK conditioned media was abolished by erlotinib while AZD4547 had relatively little effect (Fig. 5C–D). Together, these results suggest that NOK mediated activation of CSC phenotypes and PI3K inhibitor insensitivity is mediated by EGFR.

DISCUSSION

HNSCC is comprised of diverse microenvironmental elements such as CAFs, extracellular matrix, immune cells, and other supporting cells that contribute to cancer proliferation, invasion, and metastasis[1,30]. Importantly, all these elements are present and are co-treated with systemic anti-cancer treatments (such as pharmaceuticals) and localized treatments (such as radiation therapy). Tobacco consumption is a major risk factor for HNSCC, as its daily use and constant mutational insults induce a “cancerized field” of preneoplastic keratinocytes[1,3]. The cancerized field and histologically normal epithelium are increasingly being recognized as active contributors to HNSCC metastasis and therapy resistance[31,32]. Here, we used an *in vitro* co-culture model of the cancerized field and show its EGFR-dependent pro-tumorigenic role in (i) increasing proliferation and survival of neighboring HNSCC cells, (ii) blunting HNSCC therapeutic response to PI3K inhibitor, and (iii) increasing HNSCC cancer stem cell properties.

The EGFR inhibitor cetuximab is FDA approved to treat HNSCC, however many patients are refractory to anti-EGFR treatment alone or develop drug resistance[33–35]. Consequently, several preclinical studies and clinical trials have proposed combining EGFR inhibitors with PI3K inhibitors for superior anti-cancer activity. These studies show similar results to ours, but with different mechanistic explanations. Preclinical models have demonstrated upregulation of PI3K/Akt signaling in cetuximab resistant HNSCC cells and synergistic anti-cancer activity when combining cetuximab with PI3K/Akt inhibitors in mice and cell lines[36,37]. Similarly, loss of the *PTEN* tumor suppressor gene or mutation/amplification of *PIK3CA*, both of which lead to activated PI3K signaling, is associated with cetuximab resistance *in vitro* and *in vivo*[33,35,38,39]. HNSCC patients who progressed on cetuximab therapy benefitted from BKM120 + cetuximab treatment in a phase I clinical trial[40], although another clinical trial found no clinical benefit when using a similar treatment strategy[41]. Our results demonstrate that PI3K inhibition induces upregulation of EGFR

(and FGFR) ligands in both preneoplastic and HNSCC cells. As such, there are at least two benefits to therapeutically targeting both EGFR and PI3K. Firstly, to counter EGFR activation induced by PI3K inhibitor as demonstrated in this study and secondly, to combat resistance to EGFR inhibitor mediated by PI3K activation as discussed in other studies mentioned above. It is important to note that while our results demonstrate that the cancerized field induces EGFR-dependent effects in the HNSCC cell lines used, it is possible that FGFR-amplified HNSCC may respond to FGFR ligands released from precancerous keratinocytes. Additionally, our results suggest a novel feedback mechanism of RTK activation, via ligands, which has been previously observed through FOXO-induced transcription of RTK genes in PI3K inhibitor treated cells[42,43]. Thus, the benefit of this combination therapy has multiple, non-redundant mechanistic explanations.

Our study provides proof of principle that studying factors released by the cancerized field may provide insight to how tumors acquire resistance to targeted drugs, such as PI3K inhibitors. Although these findings present a novel function of the cancerized field, they bear resemblance to other studies on microenvironmental factors affecting cancer cells. For example, senescent cells are known to develop secretory activities that change the TME to favor tumorigenesis and confer resistance to therapy[44,45]. While preneoplastic keratinocytes are not necessarily senescent, repeated chemical or radiation-induced insult can initiate growth arrest or senescence in the cancerized field and may alter their secretory phenotype. In addition to the growth factors that the precancerous field can release as shown in the present study, other studies have shown that precancerous cells can secrete immunosuppressive cytokines and vasculogenic factors in models of cervical cancer and lymphoma respectively[46,47]. For HNSCC specifically, premalignant oral lesions can release inflammatory cytokines that cause localized immune skewing which could be either pro- or anti- tumorigenic[48,49]. Indeed, our proteomics results identified several quantitative differences in cytokines and chemokines in the conditioned media comparing preneoplastic keratinocytes and HNSCC cells and their responsiveness to PI3K inhibition but were outside the scope of this cell culture model. However, further exploration of the secretory phenotype of the preneoplastic field could improve therapeutic success using known agents while also leading to the development of new preventive treatments. For example, modeling the cancerized field *in vivo* to determine its influence on cytokines and immune cells within the TME may shed critical insight on HNSCC progression, relapse and response to immune-targeted therapies.

The significance of studying the cancerized field and response to PI3K inhibition is further underscored by recent successes of immune checkpoint blockade in reversing T-cell exhaustion in multiple cancers, including HNSCC, and the critical role of PI3K signaling in immune cells[50–54]. Importantly, PI3K signaling plays a key role in modulating both the adaptive and innate immune system with two catalytic subunits, PI3Kγ and PI3Kδ, being especially important in controlling leukocyte function and representing promising therapeutic targets due to their high expression in immune cells[54]. For example, inhibition of PI3Kδ in animal models of lung cancer, breast cancer, and melanoma has been shown to induce tumor regression by enhancing cytotoxic T cell function and dampening the immunosuppressive activity of regulatory T cells[55]. Similarly, PI3Kγ has been reported to promote myeloid cell-mediated angiogenesis and immunosuppression in both breast

cancer and HNSSC animal models[56,57]. Other ways the PI3K signaling pathway regulates the immune system include controlling levels of immune checkpoint ligands, such as PD-L1, and inducing MHC class I and class II expression, which may translate to increased antigen recognition and superior activity when a PI3K inhibitor is combined with immunotherapies[58,59]. In this regard, identifying targetable mechanisms of resistance and survival mediated by the cancerized field, such as through PI3K inhibition, would guide logical, effective treatment strategies. Furthermore, characterizing distinct genetic and secretory signatures of the cancerized field may be a powerful predictive biomarker for treatment or prevention of HNSCC.

Considering recent reports linking PI3K activation and cancer stem cell (CSC) properties[20,21], we hypothesized that the cancerized field may also influence CSC activity. Indeed, our data shows that factors secreted by NOK cells support a more CSC-like phenotype in recipient cancer cells. Interestingly, our tumorsphere data suggests that PI3K inhibition alone is not enough to reduce the stemness of cancer cells nourished with factors secreted by NOK cells; instead, these results are dependent upon the conditioning of NOK cells in the presence of PI3K inhibitor as media conditioned by NOK cells that had PI3K inhibitor added in afterwards fully blunted tumorsphere formation. Such secreted factors may explain the paradox in PI3K supporting CSC initiation in studies discussed above and PI3K inhibitors' inability to reduce CSC phenotypes in our model[21]. It is important to highlight that in the clinical settings, tumor and the adjacent precancerous field are treated simultaneously (in the context of systemic small molecule inhibitors). Similar to how kinase inhibitors can activate a therapy-induced secretome in tumor cells that promotes tumor growth and drug resistance[60] our data shows that treatment of NOK cells with PI3K inhibitor induces changes in their secretome that are crucial for providing pro-tumor functions such as conferring stemness. Given the common association of the cancerized field with relapse following surgery[2,4,6], our data provide an additional mechanism by which tumor cells may survive, proliferate, and recapitulate tumor heterogeneity. Although we focus on EGFR and FGFR ligands in this study, it is likely that the secreted signals from precancerous cells following PI3K inhibition involves a complex network of signals that warrants more comprehensive analysis. Studying additional factors released by the precancerous field that influence adjacent HNSCC, especially those that arise in response to kinase inhibitors commonly used in the clinic, is therefore crucial to understanding mechanisms of tumor relapse and drug resistance. Moreover, other precancer cell cultures derived from human preneoplastic lesions exist as models of the precancerous field[23]. While these cell cultures share genetic alterations similar to NOK cells, such as loss of *CDKN2A*/p16^{Ink4A} and mutations in *TP53*/p53, a thorough comparison of the effects these lines have on HNSCC cells and generation of *in vivo* models would allow for greater confidence in conclusions drawn from *in vitro* models of field cancerization.

While the preneoplastic field is known to contribute to relapse by undergoing malignant transformation, the signaling events occurring between the cancerized field, tumor, microenvironment, and their consequences is a topic of active research. Our data provide evidence that factors secreted by the cancerized field stimulates proliferation of neighboring HNSCC, increases resistance to PI3K inhibition, and enhances their cancer stem cell traits. In this regard, the cancerized field serves not only as a potential source of primary tumor

formation; rather, the cancerized field also plays an active role in the TME by supporting neighboring HNSCC and influencing therapy responsiveness.

Supplementary Material

Refer to Web version on PubMed Central for supplementary material.

ACKNOWLEDGEMENTS

Flow cytometry was performed at the University of Colorado Cancer Center Flow Cytometry Shared Resource. SOMAscan 1.3k was performed at the University of Colorado Cancer Center Genomics and Microarray Shared Resource. IncuCyte ZOOM live cell imaging and analysis was performed at the University of Colorado Cell Technologies Shared Resource. These three shared resources are funded in part by Cancer Center Support Grant P30CA046934.

FINANCIAL SUPPORT

CDY was supported by ACS IRG #16–184-56 from the American Cancer Society to the University of Colorado Cancer Center and pilot awards from the Cancer League of Colorado (AWD-163274-CY) and the University of Colorado Head and Neck Cancer Research Program. CDY, AJ and XJW were supported by SPORE P50CA261605. This work was also supported by NIH R01 DE24371 to XJW and AJ, DE027329 and DE028420 to XJW. XJW is the recipient of a Research Career Scientist award (# IK6BX005962) from the Department of Veterans Affairs and also supported by VA merit award I01 BX003232. Three University of Colorado Cancer Center shared resources utilized in this study were funded in part by Cancer Center Support Grant P30CA046934.

ABBREVIATIONS

ANOVA	Analysis of variance
APC	Allophycocyanin
BSA	Bovine serum albumin
CSC	Cancer stem cell
DMEM	Dulbecco’s modified eagle media
DMSO	Dimethyl sulfoxide
EGFR	Epidermal growth factor receptor
FBS	Fetal bovine serum
FCB	Flow cytometry buffer
FGFR	Fibroblast growth factor receptor
GFP	Green fluorescent protein
HNSCC	Head and neck squamous cell carcinoma
PBS	Phosphate buffered saline
PES	Polyethersulfone
PI3K	Phosphoinositide 3-kinase

SORE6	SOX2/OCT4 response element (six concatenated repeats)
SRB	Sulforhodamine B
TBS	Tris buffered saline
TBST	Tris buffered saline containing 0.1% Tween-20
TME	Tumor microenvironment
RIPA	Radio Immunoprecipitation Assay

REFERENCES

1. Johnson DE, Burtness B, Leemans CR, Lui VWY, Bauman JE, Grandis JR. Head and neck squamous cell carcinoma. Nat Rev Dis Primers. 2020;6(1):92. [PubMed: 33243986]
2. Califano J, van der Riet P, Westra W, et al. Genetic progression model for head and neck cancer: implications for field cancerization. Cancer research. 1996;56(11):2488–2492. [PubMed: 8653682]
3. Leemans CR, Braakhuis BJ, Brakenhoff RH. The molecular biology of head and neck cancer. Nature reviews Cancer. 2011;11(1):9–22. [PubMed: 21160525]
4. Mohan M, Jagannathan N. Oral field cancerization: an update on current concepts. Oncol Rev. 2014;8(1):244. [PubMed: 25992232]
5. Tabor MP, Brakenhoff RH, van Houten VM, et al. Persistence of genetically altered fields in head and neck cancer patients: biological and clinical implications. Clinical cancer research : an official journal of the American Association for Cancer Research. 2001;7(6):1523–1532. [PubMed: 11410486]
6. Curtius K, Wright NA, Graham TA. An evolutionary perspective on field cancerization. Nature reviews Cancer. 2018;18(1):19–32. [PubMed: 29217838]
7. Lui VW, Hedberg ML, Li H, et al. Frequent mutation of the PI3K pathway in head and neck cancer defines predictive biomarkers. Cancer discovery. 2013;3(7):761–769. [PubMed: 23619167]
8. Chung CH, Guthrie VB, Masica DL, et al. Genomic alterations in head and neck squamous cell carcinoma determined by cancer gene-targeted sequencing. Ann Oncol. 2015;26(6):1216–1223. [PubMed: 25712460]
9. Stransky N, Egloff AM, Tward AD, et al. The mutational landscape of head and neck squamous cell carcinoma. Science. 2011;333(6046):1157–1160. [PubMed: 21798893]
10. Cancer Genome Atlas N. Comprehensive genomic characterization of head and neck squamous cell carcinomas. Nature. 2015;517(7536):576–582. [PubMed: 25631445]
11. Soulieres D, Faivre S, Mesia R, et al. Buparlisib and paclitaxel in patients with platinum-pretreated recurrent or metastatic squamous cell carcinoma of the head and neck (BERIL-1): a randomised, double-blind, placebo-controlled phase 2 trial. Lancet Oncol 2017;18(3):323–335. [PubMed: 28131786]
12. Schmid P, Pinder SE, Wheatley D, et al. Phase II Randomized Preoperative Window-of-Opportunity Study of the PI3K Inhibitor Pictilisib Plus Anastrozole Compared With Anastrozole Alone in Patients With Estrogen Receptor-Positive Breast Cancer. J Clin Oncol. 2016;34(17):1987–1994. [PubMed: 26976426]
13. Baselga J, Im SA, Iwata H, et al. Buparlisib plus fulvestrant versus placebo plus fulvestrant in postmenopausal, hormone receptor-positive, HER2-negative, advanced breast cancer (BELLE-2): a randomised, double-blind, placebo-controlled, phase 3 trial. Lancet Oncol. 2017;18(7):904–916. [PubMed: 28576675]
14. Keysar SB, Astling DP, Anderson RT, et al. A patient tumor transplant model of squamous cell cancer identifies PI3K inhibitors as candidate therapeutics in defined molecular bins. Mol Oncol. 2013;7(4):776–790. [PubMed: 23607916]
15. Ma CX, Luo J, Naughton M, et al. A Phase I Trial of BKM120 (Buparlisib) in Combination with Fulvestrant in Postmenopausal Women with Estrogen Receptor-Positive Metastatic Breast Cancer.

Clinical cancer research : an official journal of the American Association for Cancer Research. 2016;22(7):1583–1591. [PubMed: 26563128]

16. Mayer IA, Abramson VG, Isakoff SJ, et al. Stand up to cancer phase Ib study of pan-phosphoinositide-3-kinase inhibitor buparlisib with letrozole in estrogen receptor-positive/human epidermal growth factor receptor 2-negative metastatic breast cancer. J Clin Oncol. 2014;32(12):1202–1209. [PubMed: 24663045]
17. Chen D, Wu M, Li Y, et al. Targeting BMI1(+) Cancer Stem Cells Overcomes Chemoresistance and Inhibits Metastases in Squamous Cell Carcinoma. Cell Stem Cell. 2017;20(5):621–634 e626. [PubMed: 28285905]
18. Nguyen LV, Vanner R, Dirks P, Eaves CJ. Cancer stem cells: an evolving concept. Nature reviews Cancer. 2012;12(2):133–143. [PubMed: 22237392]
19. Chen SMY, Li B, Nicklawsky AG, et al. Deletion of p53 and Hyper-Activation of PIK3CA in Keratin-15(+) Stem Cells Lead to the Development of Spontaneous Squamous Cell Carcinoma. Int J Mol Sci. 2020;21(18).
20. Keysar SB, Le PN, Miller B, et al. Regulation of Head and Neck Squamous Cancer Stem Cells by PI3K and SOX2. J Natl Cancer Inst. 2017;109(1).
21. Chen X, Cao Y, Sedhom W, et al. Distinct roles of PIK3CA in the enrichment and maintenance of cancer stem cells in head and neck squamous cell carcinoma. Mol Oncol. 2020;14(1):139–158. [PubMed: 31600013]
22. Martin D, Abba MC, Molinolo AA, et al. The head and neck cancer cell oncogenome: a platform for the development of precision molecular therapies. Oncotarget. 2014;5(19):8906–8923. [PubMed: 25275298]
23. de Boer DV, Brink A, Buijze M, et al. Establishment and Genetic Landscape of Precancer Cell Model Systems from the Head and Neck Mucosal Lining. Mol Cancer Res. 2019;17(1):120–130. [PubMed: 30224542]
24. Hernandez AL, Young CD, Bian L, et al. PARP Inhibition Enhances Radiotherapy of SMAD4-Deficient Human Head and Neck Squamous Cell Carcinomas in Experimental Models. Clinical cancer research : an official journal of the American Association for Cancer Research. 2020;26(12):3058–3070. [PubMed: 32139402]
25. Zhao M, Sano D, Pickering CR, et al. Assembly and initial characterization of a panel of 85 genomically validated cell lines from diverse head and neck tumor sites. Clinical cancer research : an official journal of the American Association for Cancer Research. 2011;17(23):7248–7264. [PubMed: 21868764]
26. Tang B, Raviv A, Esposito D, et al. A flexible reporter system for direct observation and isolation of cancer stem cells. Stem Cell Reports. 2015;4(1):155–169. [PubMed: 25497455]
27. Gomez KE, Wu F, Keysar SB, et al. Cancer Cell CD44 Mediates Macrophage/Monocyte-Driven Regulation of Head and Neck Cancer Stem Cells. Cancer research. 2020;80(19):4185–4198. [PubMed: 32816856]
28. Moyer JD, Barbacci EG, Iwata KK, et al. Induction of apoptosis and cell cycle arrest by CP-358,774, an inhibitor of epidermal growth factor receptor tyrosine kinase. Cancer research. 1997;57(21):4838–4848. [PubMed: 9354447]
29. Gavine PR, Mooney L, Kilgour E, et al. AZD4547: an orally bioavailable, potent, and selective inhibitor of the fibroblast growth factor receptor tyrosine kinase family. Cancer research. 2012;72(8):2045–2056. [PubMed: 22369928]
30. Chen SMY, Krinsky AL, Woolaver RA, Wang X, Chen Z, Wang JH. Tumor immune microenvironment in head and neck cancers. Mol Carcinog. 2020;59(7):766–774. [PubMed: 32017286]
31. Mazilu L, Suceveanu AI, Stanculeanu DL, Gheorghe AD, Fricatel G, Negru SM. Tumor microenvironment is not an ‘innocent bystander’ in the resistance to treatment of head and neck cancers (Review). Exp Ther Med. 2021;22(4):1128. [PubMed: 34466142]
32. Singh P, Banerjee R, Piao S, et al. Squamous cell carcinoma subverts adjacent histologically normal epithelium to promote lateral invasion. J Exp Med. 2021;218(6).
33. Leblanc O, Vacher S, Lecerf C, et al. Biomarkers of cetuximab resistance in patients with head and neck squamous cell carcinoma. Cancer Biol Med. 2020;17(1):208–217. [PubMed: 32296588]

34. Vermorken JB, Trigo J, Hitt R, et al. Open-label, uncontrolled, multicenter phase II study to evaluate the efficacy and toxicity of cetuximab as a single agent in patients with recurrent and/or metastatic squamous cell carcinoma of the head and neck who failed to respond to platinum-based therapy. J Clin Oncol. 2007;25(16):2171–2177. [PubMed: 17538161]
35. Eze N, Lee JW, Yang DH, et al. PTEN loss is associated with resistance to cetuximab in patients with head and neck squamous cell carcinoma. Oral Oncol. 2019;91:69–78. [PubMed: 30926065]
36. Zaryouh H, De Pauw I, Baysal H, et al. The Role of Akt in Acquired Cetuximab Resistant Head and Neck Squamous Cell Carcinoma: An In Vitro Study on a Novel Combination Strategy. Front Oncol. 2021;11:697967. [PubMed: 34568028]
37. Klinghammer K, Politz O, Eder T, et al. Combination of copanlisib with cetuximab improves tumor response in cetuximab-resistant patient-derived xenografts of head and neck cancer. Oncotarget. 2020;11(41):3688–3697. [PubMed: 33110476]
38. Izumi H, Wang Z, Goto Y, et al. Pathway-Specific Genome Editing of PI3K/mTOR Tumor Suppressor Genes Reveals that PTEN Loss Contributes to Cetuximab Resistance in Head and Neck Cancer. Molecular cancer therapeutics. 2020;19(7):1562–1571. [PubMed: 32430488]
39. Psyrri A, Lee JW, Pectasides E, et al. Prognostic biomarkers in phase II trial of cetuximab-containing induction and chemoradiation in resectable HNSCC: Eastern cooperative oncology group E2303. Clinical cancer research : an official journal of the American Association for Cancer Research. 2014;20(11):3023–3032. [PubMed: 24700741]
40. Brisson RJ, Kochanny S, Arshad S, et al. A pilot study of the pan-class I PI3K inhibitor buparlisib in combination with cetuximab in patients with recurrent or metastatic head and neck cancer. Head & neck. 2019;41(11):3842–3849. [PubMed: 31486207]
41. Jimeno A, Shirai K, Choi M, et al. A randomized, phase II trial of cetuximab with or without PX-866, an irreversible oral phosphatidylinositol 3-kinase inhibitor, in patients with relapsed or metastatic head and neck squamous cell cancer. Ann Oncol. 2015;26(3):556–561. [PubMed: 25524478]
42. Chandarlapaty S, Sawai A, Scaltriti M, et al. AKT inhibition relieves feedback suppression of receptor tyrosine kinase expression and activity. Cancer Cell. 2011;19(1):58–71. [PubMed: 21215704]
43. Chakrabarty A, Sanchez V, Kuba MG, Rinehart C, Arteaga CL. Breast Cancer Special Feature: Feedback upregulation of HER3 (ErbB3) expression and activity attenuates antitumor effect of PI3K inhibitors. Proc Natl Acad Sci U S A. 2011.
44. Schoetz U, Klein D, Hess J, et al. Early senescence and production of senescence-associated cytokines are major determinants of radioresistance in head-and-neck squamous cell carcinoma. Cell Death Dis. 2021;12(12):1162. [PubMed: 34911941]
45. Faget DV, Ren Q, Stewart SA. Unmasking senescence: context-dependent effects of SASP in cancer. Nature reviews Cancer. 2019;19(8):439–453. [PubMed: 31235879]
46. Demoulin SA, Somja J, Duray A, et al. Cervical (pre)neoplastic microenvironment promotes the emergence of tolerogenic dendritic cells via RANKL secretion. Oncoimmunology. 2015;4(6):e1008334. [PubMed: 26155412]
47. Shen R, Ye Y, Chen L, Yan Q, Barsky SH, Gao JX. Precancerous stem cells can serve as tumor vasculogenic progenitors. PLoS One. 2008;3(2):e1652. [PubMed: 18286204]
48. Woodford D, Johnson SD, De Costa AM, Young MR. An Inflammatory Cytokine Milieu is Prominent in Premalignant Oral Lesions, but Subsides when Lesions Progress to Squamous Cell Carcinoma. J Clin Cell Immunol. 2014;5(3).
49. Johnson SD, Levingston C, Young MR. Premalignant Oral Lesion Cells Elicit Increased Cytokine Production and Activation of T-cells. Anticancer research. 2016;36(7):3261–3270. [PubMed: 27354582]
50. Pardoll DM. The blockade of immune checkpoints in cancer immunotherapy. Nature reviews Cancer. 2012;12(4):252–264. [PubMed: 22437870]
51. Bauman JE, Cohen E, Ferris RL, et al. Immunotherapy of head and neck cancer: Emerging clinical trials from a National Cancer Institute Head and Neck Cancer Steering Committee Planning Meeting. Cancer. 2017;123(7):1259–1271. [PubMed: 27906454]

52. Ferris RL, Blumenschein G Jr., Fayette J, et al. Nivolumab for Recurrent Squamous-Cell Carcinoma of the Head and Neck. The New England journal of medicine. 2016;375(19):1856–1867. [PubMed: 27718784]

53. Burtness B, Harrington KJ, Greil R, et al. Pembrolizumab alone or with chemotherapy versus cetuximab with chemotherapy for recurrent or metastatic squamous cell carcinoma of the head and neck (KEYNOTE-048): a randomised, open-label, phase 3 study. Lancet. 2019;394(10212):1915–1928. [PubMed: 31679945]

54. Okkenhaug K Signaling by the phosphoinositide 3-kinase family in immune cells. Annual review of immunology. 2013;31:675–704.

55. Ali K, Soond DR, Pineiro R, et al. Inactivation of PI(3)K p110delta breaks regulatory T-cell-mediated immune tolerance to cancer. Nature. 2014;510(7505):407–411. [PubMed: 24919154]

56. Kaneda MM, Messer KS, Ralainirina N, et al. PI3Kgamma is a molecular switch that controls immune suppression. Nature. 2016;539(7629):437–442. [PubMed: 27642729]

57. Schmid MC, Avraamides CJ, Dippold HC, et al. Receptor tyrosine kinases and TLR/IL1Rs unexpectedly activate myeloid cell PI3kgamma, a single convergent point promoting tumor inflammation and progression. Cancer Cell. 2011;19(6):715–727. [PubMed: 21665146]

58. Chandrasekaran S, Sasaki M, Scharer CD, et al. Phosphoinositide 3-Kinase Signaling Can Modulate MHC Class I and II Expression. Mol Cancer Res. 2019;17(12):2395–2409. [PubMed: 31548239]

59. Lastwika KJ, Wilson W 3rd, Li QK, et al. Control of PD-L1 Expression by Oncogenic Activation of the AKT-mTOR Pathway in Non-Small Cell Lung Cancer. Cancer research. 2016;76(2):227–238. [PubMed: 26637667]

60. Obenauf AC, Zou Y, Ji AL, et al. Therapy-induced tumour secretomes promote resistance and tumour progression. Nature. 2015;520(7547):368–372. [PubMed: 25807485]

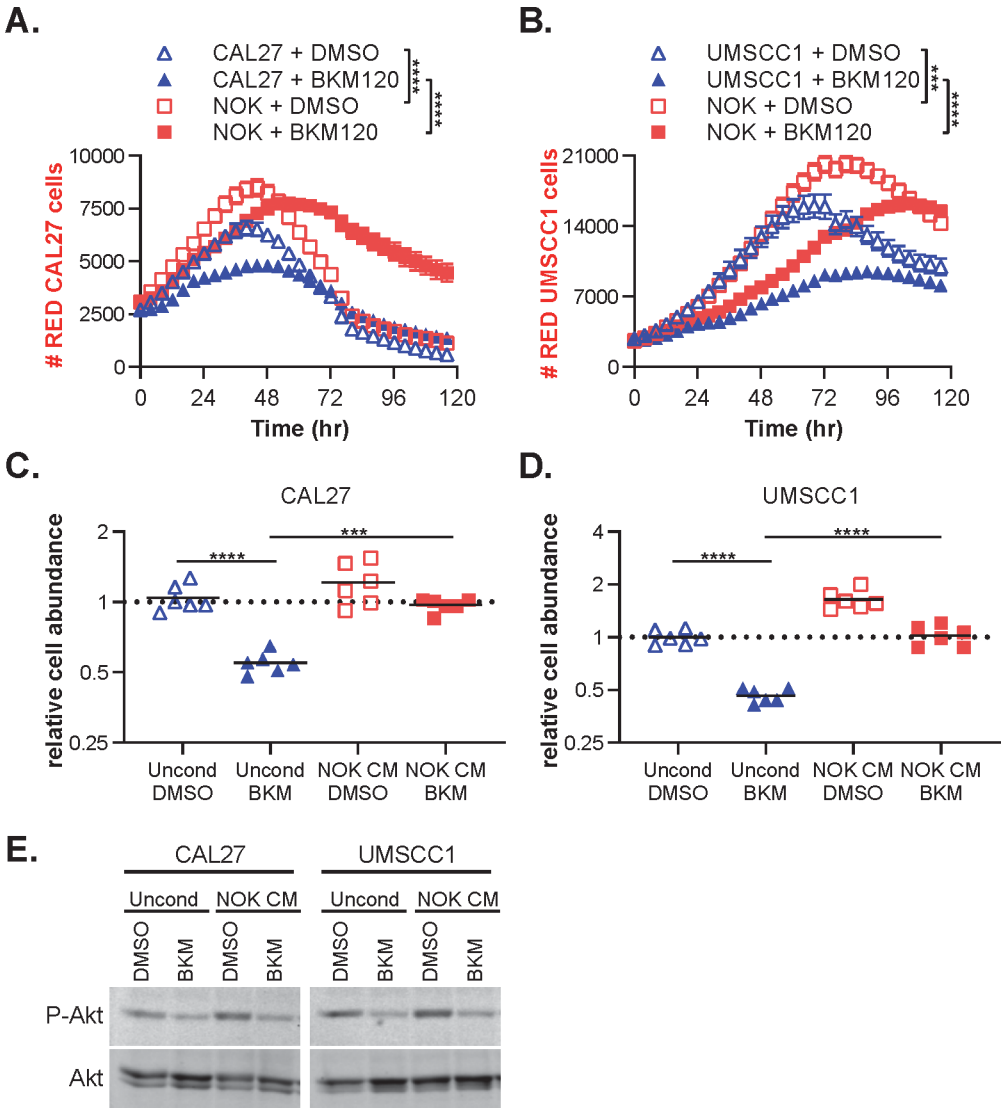

Figure 1: NOK cells increase the proliferation and survival of PI3K inhibitor-treated HNSCC cells.

A) Nuclear red labelled CAL27 cells were co-cultured with an equal number of unlabeled CAL27 or unlabeled NOK cells in low serum media and treated with DMSO or 1 mM BKM120. The # of nuclear red CAL27 cells was monitored by IncuCyte real time imaging. **B)** Same as panel A, but utilizing nuclear red labeled UMSCC1 cells. ***: $p<0.001$; ****: $p<0.0001$ by repeated measures ANOVA with Tukey's multiple comparison test. **C-D)** The low serum media conditioned by NOK cells treated with DMSO or 2 mM BKM120 (NOK CM) was harvested and applied to an equal volume of recipient CAL27 cells **(C)** or UMSCC1 cells **(D)**. Unconditioned low serum media (Uncond) containing DMSO or BKM120 was used as a control. Relative abundance of recipient cells was quantified after three days of culture using SRB assay, normalized to the DMSO-containing unconditioned media treatment. ***: $p<0.001$; ****: $p<0.0001$ by one way ANOVA with Tukey's multiple comparison test. **E)** Recipient CAL27 or UMSC1 cells treated as described in panels C-D were lysed after three days treatment. Lysates were subjected to immunoblot analysis using

the indicated antibodies. Each experiment was repeated 2 or more times with similar results and one representative experiment is presented.

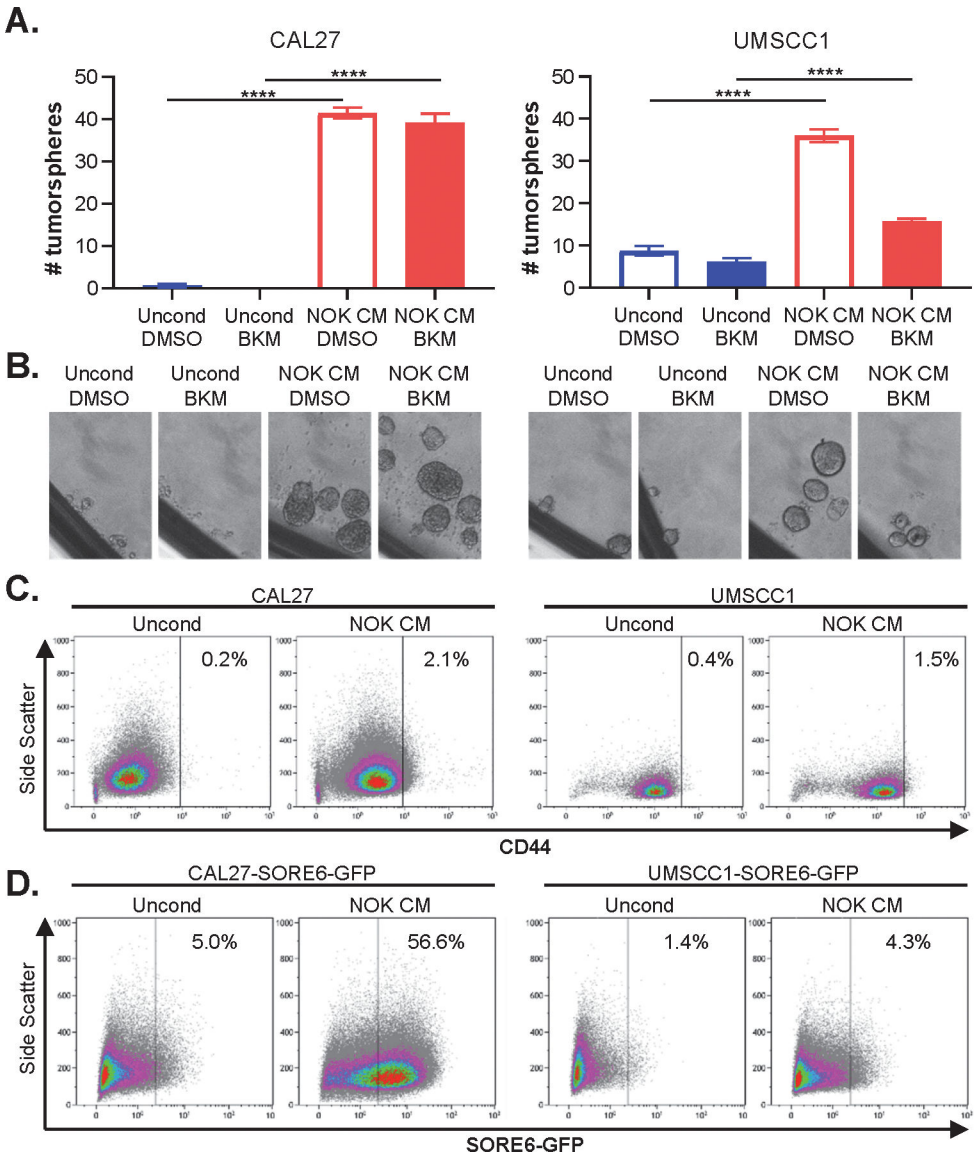

Figure 2: Factors released by NOK cells increase cancer stem cell traits in recipient HNSCC cells.

A-B) The low serum media conditioned by NOK cells treated with DMSO or 2 mM BKM120 (NOK CM) was harvested and applied to 200 recipient CAL27 or UMSCC1 seeded in ultralow attachment plates. The number of tumorspheres > 50 μm per well was counted on day 10 **(A)** and representative images are presented **(B)**. Unconditioned low serum media (Uncond) containing DMSO or 1 mM BKM120 was used as a control. ****: $p<0.0001$ by one way ANOVA with Tukey's multiple comparison test. **C)** Recipient CAL27 or UMSC1 tumorspheres treated as described in panels A-B for three days were dissociated into single cells, stained with anti-CD44 antibody, and analyzed by FACS to determine the percentage of $CD44^{high}$ cells. **D)** Recipient CAL27-SORE6-GFP or UMSCC1-SORE6-GFP were treated and harvested as described in panel C and evaluated for SORE6-dependent GFP expression. Each experiment was repeated 2 or more times with similar results and one representative experiment is presented.

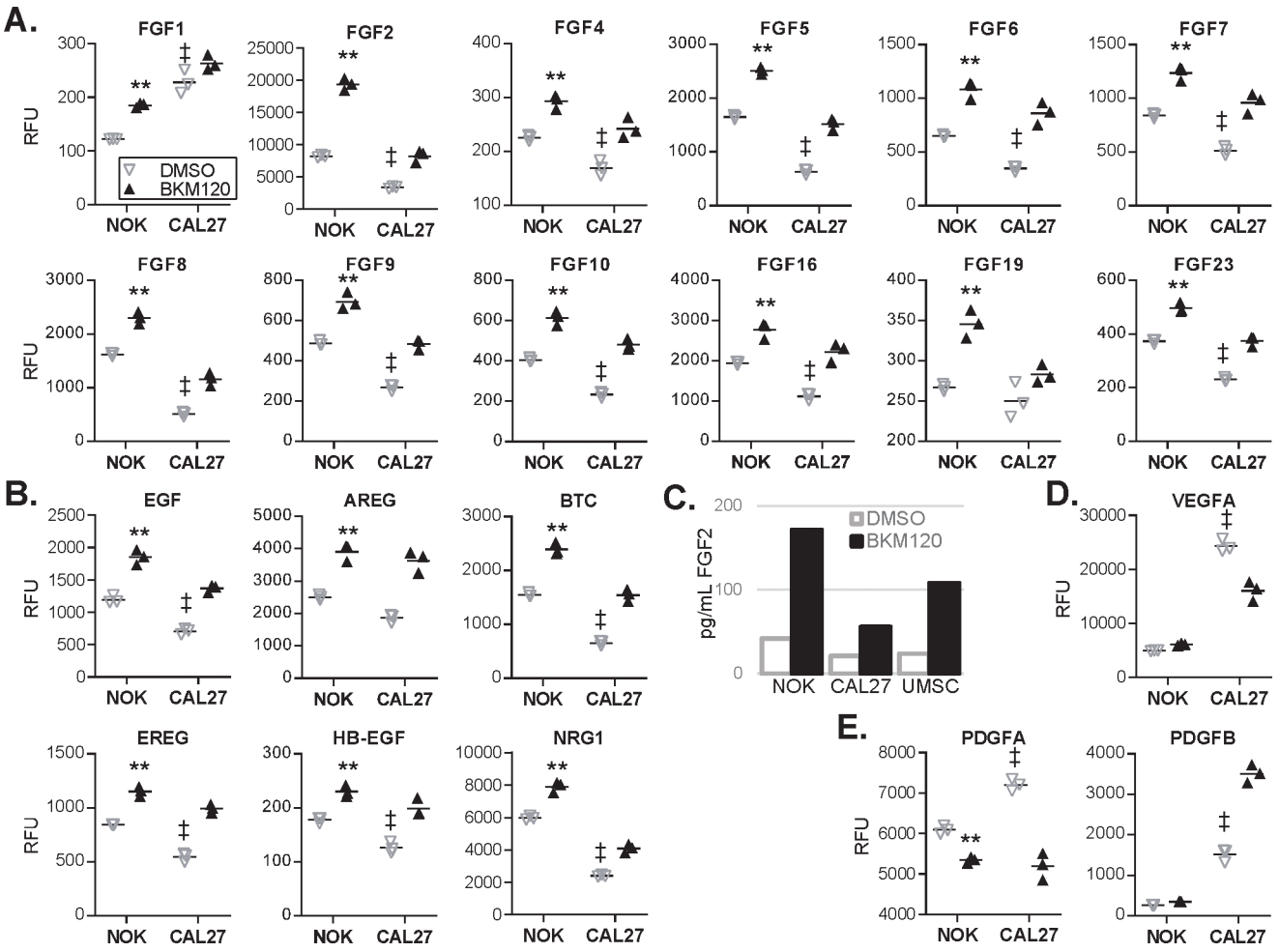

Figure 3: NOK cells have elevated levels of FGFR and EGFR ligands that are increased by PI3K inhibition.

NOK or CAL27 cells were serum starved 24 hr then treated another 24 hr with DMSO or 1 mM BKM120. Conditioned media was harvested, clarified by centrifugation and the relative abundance of >1,300 analytes determined by SOMAscan analysis. Representative ligands for the following RTK families are presented: **A)** FGFR family; **B)** EGFR family; **C)** PDGFR family**; D)** VEGFR family. ** p<0.01 (DMSO vs BKM120), ‡ p<0.01 (NOK vs CAL27) by two-way ANOVA with Tukey's multiple comparison test. **E)** ELISA analysis of FGF2 levels in serum free conditioned media harvested from NOK, CAL27 or UMSCC1 cells.

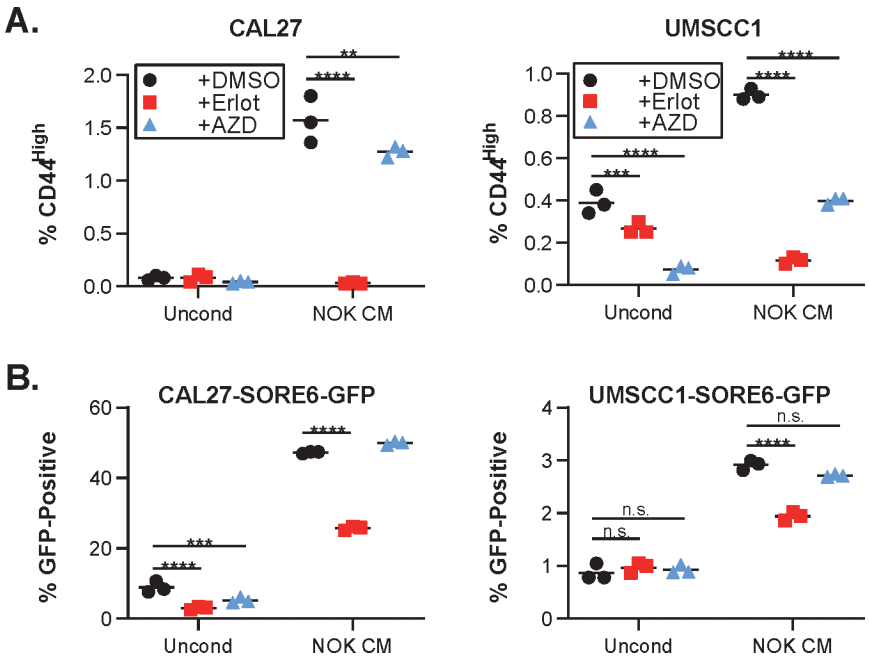

Figure 4: The cancer stem cell traits conferred by NOK cells to recipient HNSCC cells is EGFR dependent.

A) The low serum media conditioned by NOK cells (NOK CM) or unconditioned low serum media (Uncond) was harvested and applied to recipient CAL27 or UMSCC1 cells seeded in ultralow attachment plates and supplemented with DMS0, 0.5 mM Erlotonib (Erlot) or 0.5 mM AZD4547 (AZD). Tumorspheres were dissociated into single cells three days later, stained with anti-CD44 antibody and analyzed by FACS to determine the percentage of $CD44^{high}$ cells. **B)** Recipient CAL27-SORE6-GFP or UMSCC1-SORE6-GFP were treated and harvested as described in panel A and evaluated for SORE6-dependent GFP expression. **: p<0.01; ***: p<0.001; ****: p<0.0001 by two-way ANOVA with Tukey's multiple comparison test. Each experiment was repeated 2 or more times with similar results and one representative experiment is presented.

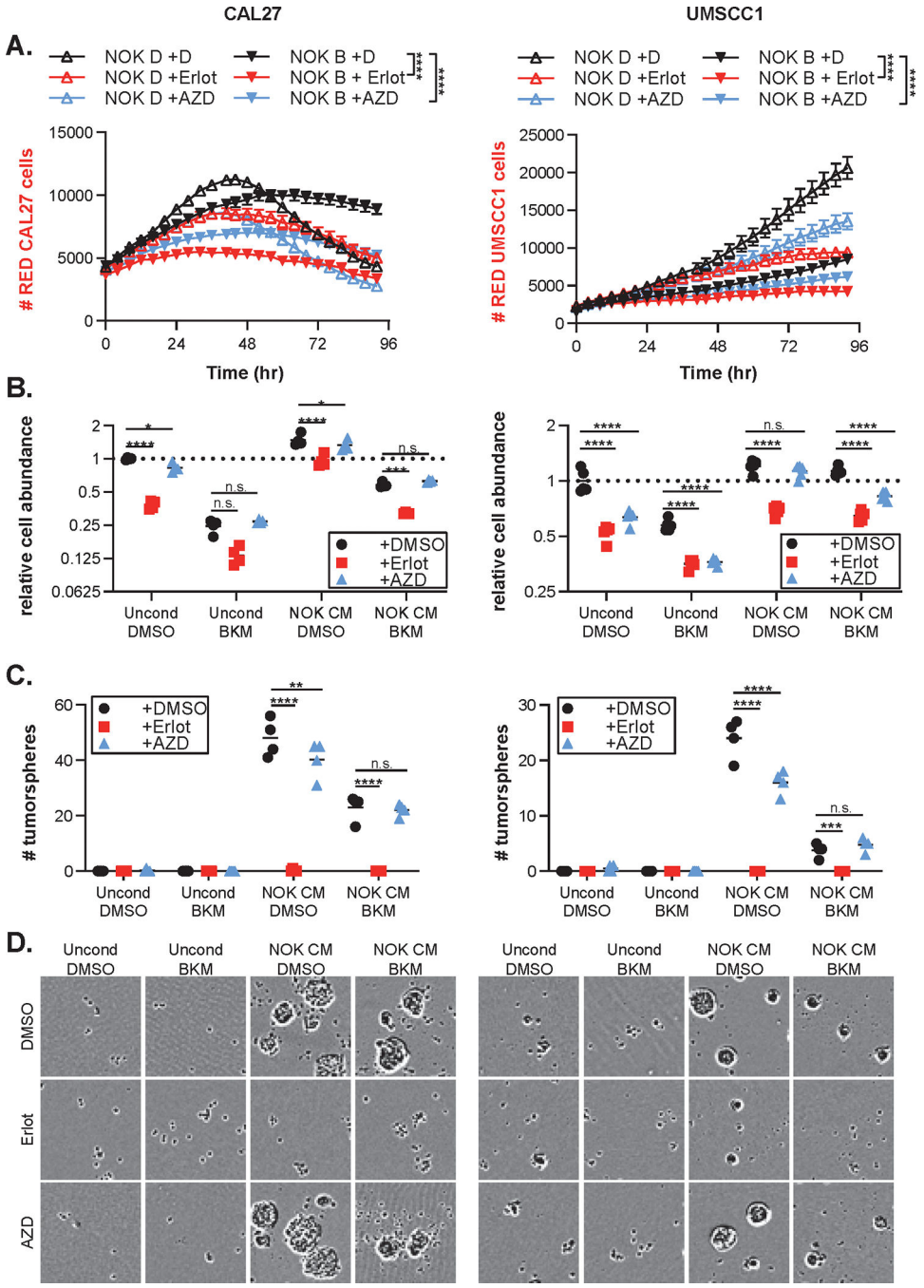

Figure 5: BKM120 insensitivity and tumorsphere promotion conferred by NOK cells to HNSCC cells is EGFR-dependent.

A) Nuclear red labelled CAL27 or UMSCC1 cells were co-cultured with an equal number of unlabeled NOK cells in low serum media and treated with DMSO (D) or 1 mM BKM120 (B) plus DMSO, 0.5 mM Erlotonib (Erlot) or 0.5 mM AZD4547 (AZD). The # of nuclear red cells was monitored by IncuCyte real time imaging. ****: $p<0.0001$ by repeated measures ANOVA with Tukey's multiple comparison test. **B)** The low serum media conditioned by NOK cells treated with DMSO or 2 mM BKM120 (NOK CM) or parallel

unconditioned media (Uncond) was harvested. DMSO, 1 mM Erlotonib (Erlot) or 1 mM AZD4547 was added to these media and applied to an equal volume of recipient CAL27 or UMSCC1 cells, cutting drug concentrations in half. Relative abundance of recipient cells was quantified after three days of culture using SRB assay, normalized to the DMSO-containing unconditioned media treatment. *: $p<0.05$; ***: $p<0.001$; ****: $p<0.0001$ by two-way ANOVA with Tukey's multiple comparison test. **C-D)** 200 recipient CAL27 or UMSC1 cells treated as described in panels B, but in ultralow attachment plates with B27 supplement to assess tumor sphere formation. The number of tumorspheres per well is quantified in panel C and representative pictures in panel D. Each experiment was repeated 2 or more times with similar results and one representative experiment is presented.

Table 1:

Antibody List

Antigen	Manufacturer	Catalog #	Use	Dilution
Akt	Cell Signaling	#4685	IB	1:1,000
P-Akt (Ser473)	Cell Signaling	#4060	IB	1:1,000
Sox2	Cell Signaling	#3679	IB	1:1,000
β-Tubulin	Cell Signaling	#2128	IB	1:1,000
CD44-APC	eBioscience	17-0441-82	FC	1:40

Note: IB: immunoblot; FC: Flow Cytometry